

2 **A novel polystyrene-based scintillator** 3 **production process involving additive manufacturing**

4 **S. Berns,^{a,b,c,1} A. Boyarintsev,^{d,1} S. Hugon,^{a,b,c,1} U. Kose,^{e,1} D. Sgalaberna,^{e,*,1} A. De**
5 **Roeck,^e A. Lebedynskiy,^d T. Sibillieva,^d P. Zhmurin^d**

6 ^a*Haute Ecole Spécialisée de Suisse Occidentale (HES-SO), CH-2800 Delémont, Route de Moutier 14,*
7 *Switzerland*

8 ^b*Haute Ecole d'Ingénierie du canton de Vaud (HEIG-VD), CH-1401 Yverdon-les-Bains, Route de Cheseaux*
9 *1, Switzerland*

10 ^c*COMATEC-AddiPole, CH-1450 Sainte-Croix, Technopole de Sainte-Croix, Rue du Progrès 31, Switzerland*

11 ^d*Institute for Scintillation Materials NAS of Ukraine (ISMA), Kharkiv 61072, Ukraine*

12 ^e*European Organization for Nuclear Research (CERN), 1211 Geneva 23, Switzerland*

13 ^{*}*Now at ETH Zurich, Institute for Particle Physics and Astrophysics, CH-8093 Zurich, Switzerland*

E-mail: umut.kose@cern.ch, davide.sgalaberna@cern.ch,
14 siddhartha.berns@heig-vd.ch, sylvain.hugon@heig-vd.ch,
boyarintsev@isma.kharkov.ua

15 **ABSTRACT:** Plastic scintillator detectors are widely used in particle physics thanks to the very
16 good particle identification, tracking capabilities and time resolution. However, new experimental
17 challenges and the need for enhanced performance require the construction of detector geometries
18 that are complicated using the current production techniques. In this article we propose a new
19 production technique based on additive manufacturing that aims to 3D print polystyrene-based
20 scintillator. The production process and the results of the scintillation light output measurement of
21 the 3D-printed scintillator are reported.

22 **KEYWORDS:** Plastic scintillator, polystyrene, 3D print, additive manufacturing, particle detector

¹Corresponding author

23	Contents	
24	1 Introduction	1
25	2 Basic principles of plastic scintillator detectors	2
26	3 Plastic scintillator detectors and three-dimensional printing	2
27	3.1 Production processes	3
28	3.2 Additive manufacturing	4
29	4 3D-printing of polystyrene-based scintillator	4
30	4.1 Filament production	5
31	4.2 3D-printing process	6
32	5 Performance of the 3D printed scintillator	8
33	6 Conclusions	12

34 1 Introduction

35 Plastic scintillator detectors were developed in the early 50s [1] and are currently widely used in
36 high-energy physics, astroparticle physics as well as in many applications like muon tomography
37 and hadron therapy.

38 Plastic scintillator is composed of a mixture of carbon and hydrogen based molecules. The
39 capability of efficiently producing scintillation light by traversing charged particles makes this
40 detectors very suitable for particle identification (PID) and allows measuring the particle interaction
41 time with sub-nanosecond precision. Plastic scintillator detectors can be used for particle tracking,
42 see e.g. [2]. Depending on the granularity, such detectors can reach a spatial resolution of better
43 than 100 μm [3]. Such detectors can also perform precise calorimetric measurements if alternated
44 with layers of heavier material like iron or lead [4]. Plastic scintillator detectors are also often used
45 in neutrino experiments for the good tracking and PID capabilities, and with a large mass acting as
46 active neutrino target [5–7]. Thanks to the presence of low atomic mass nuclei, a unique feature
47 of plastic scintillator detectors is the very high neutron detection efficiency, which is particularly
48 important for neutrino experiments. Fast neutrons, with energies in the MeV range can transfer a
49 relatively large amount of energy when scattering off hydrogen protons or when breaking-up the
50 carbon nucleus, and allow for a neutron time of flight measurement [8]. If the plastic scintillator
51 is doped with, or alternated with layers composed by nuclei like lithium, boron or gadolinium,
52 neutrons can also be thermalized and efficiently captured with a resulting release of a large number
53 of photons [9].

54 All the features of plastic scintillator-based detectors described above can be achieved often by
55 implementing complex geometries which put important constraints on the production and detector

56 construction processes. In this article we describe the current state of the art of plastic scintillator
57 production and propose a new production technique based on additive manufacturing applied to
58 polystyrene-based plastic scintillator, with the goal to allow for an easy production but at the same
59 time keeping performances comparable to more standard production techniques like extrusion or
60 injection molding.

61 **2 Basic principles of plastic scintillator detectors**

62 Typically, plastic scintillator are made of polystyrene or vinyltoluene material. Molecules of an
63 activator, like paraterphenyl, are introduced into the polymer at a level of approximately 2% by
64 weight.

65 This composition practically did not undergo any changes in the last fifty years, although many
66 new polymers have been proposed. The main hurdles are the difficulty of synthesizing big scintillator
67 objects with a sufficient degree of transparency, the absence of a luminescent chromophore in their
68 composition groups, the impossibility of dissolving luminescent additives to the required amount,
69 and the large costs of synthesising the initial monomer molecules.

70 The scintillation mechanism goes through several steps. A sufficiently energetic charged par-
71 ticle interacting with the plastic scintillator excites the polymer matrix molecules. The excitation
72 energy is transferred to the activator via a resonant dipole-dipole interaction, called Foerster mech-
73 anism [10], inversely proportional to the 6-th power of the intramolecule distance. This interaction
74 strongly couples the polymer base and the activator, sharply increasing the light yield of the plastic
75 scintillator and reducing the light emission delay. The activator must provide the necessary non-
76 radiative collection of the polymer-base excitation energy in order to achieve a sufficient conversion
77 into the luminescence of the required spectral range. The most important requirement for the choice
78 of the activator molecule is the effective overlap between its absorption band and the luminescence
79 band of the polymer to ensure an efficient transfer of excitation energy. The scintillation mechanism
80 in organic materials is detailed in [11, 12]. A second dopant, called shifter, is usually added to
81 change the light wavelength to a different spectrum region to provide the maximal transparency of
82 the material to the emitted light. Fig. 1 shows schematically the mechanism via which a charged par-
83 ticle transfers part of its energy to the scintillator material and how the scintillation light is produced.

84

85 **3 Plastic scintillator detectors and three-dimensional printing**

86 The light produced by the plastic scintillator is usually in the blue band. PhotoMultipliers Tubes
87 (PMTs) or Silicon PhotoMultipliers (SiPM) can be used to count the number of photons produced.
88 They can be either directly coupled with the plastic scintillator or, in more complex geometries, the
89 light wavelength can be shifted in the wavelength shifting (WLS) fiber and shifted, for example,
90 to the green band. The WLS fiber can consequently capture the scintillation light and guide it to
91 the photocounter. The functioning of scintillating fibers, whose core is made of polystyrene-based
92 scintillator, is very similar.

93 Requirements on the performance of plastic scintillator detectors include: high scintillation
94 light yield, high transparency, fine granularity if combined with optical isolation, long-term stability

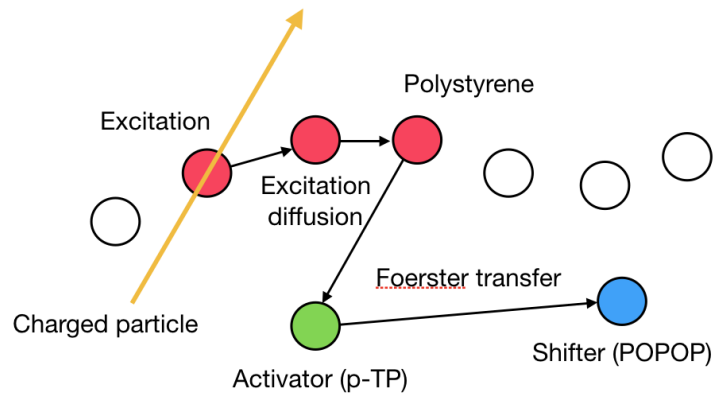


Figure 1: Energy transfer in plastic scintillator. An electron excites the polystyrene molecules that hereafter diffuse the excitation to the other molecules nearby. Through the Förster mechanism the energy is transferred to the activator molecules (e.g. p-terphenyl) that emit ultraviolet photons. A second component (e.g. 2,2- p-phenylene-bis(5-pheniloxazole)) shifts the light wavelength from ~ 340 nm to ~ 400 nm.

95 and fast scintillation light production. Recently, very fine 3D-granular plastic scintillator detectors
 96 (3D-cube scintillator) have been proposed for future neutrino detectors. One example is given by
 97 an active neutrino target detector, made of two million $10 \times 10 \times 10$ mm³ plastic-scintillator cubes,
 98 optically isolated and with three independent holes along the three orthogonal directions that host
 99 WLS fibers [13]. Future step changes in this technology may require a larger target mass combined
 100 with finer granularity. An obvious limitation is the challenge to assemble so many small cubes with
 101 the required precision.

102 3.1 Production processes

103 High-quality plastic scintillator can be produced with the cast polymerization technique [14]. A
 104 liquid monomer with dissolved dopants is poured into a mold and heated. Eventually, after cooling,
 105 a rigid solid plastic is obtained. This technique is quite expensive compared to other methods, given
 106 the rather complex technique and the relatively long production time required.

107 Another possible technique is the injection molding [15, 16]. This method is widely used in
 108 industry: optically transparent granulated polystyrene is mixed with the dopant and directed into
 109 the mold at a temperature of approximately 200°C. The quality of the plastic scintillator is inferior
 110 to the one obtained with cast polymerization, but sufficient to make particles detectors for most of
 111 the applications.

112 An alternative technique is the extrusion [17, 18]. This production method can provide plastic
 113 scintillator at very low cost but with usually poorer optical attenuation properties. It is often used
 114 for the production of very large detectors.

115 The methods described above allow to produce individual plastic scintillator components that
 116 afterward need to be assembled. However, when more complex geometries are needed, these
 117 methods may be insufficient or the assembly may become very difficult. An ideal solution would

118 consist of a production technique that fabricates all the individual plastic scintillator objects of the
119 desired geometrical shape already assembled, composing a single scintillator block, and at the same
120 time keeping all the quality characteristics high as described above.

121 **3.2 Additive manufacturing**

122 Plastic scintillator detectors are traditionally produced through the techniques described in sec. 3.1,
123 and then manufactured and adapted to the detector geometry by a subtractive process such as
124 machining or drilling. With such process it is possible to manufacture single cubes or internal
125 cells with excellent accuracy and good transparency but, depending on the final detector geometry,
126 with difficulties in the assembly or machining. Additive manufacturing (AM) opens a door to new
127 automated processes that can drastically simplify the construction of plastic scintillator detectors.

128 More commonly known as rapid prototyping or three-dimensional (3D) printing, AM processes
129 are used to design and create parts by adding material in a layer-wise fashion. AM has undergone
130 significant developments since its conception for the first commercial application for the technology,
131 known as stereolithography [19]. AM technologies are capable of fabricating parts for mass
132 customization with multiple materials and complex internal geometries. Moreover, these processes
133 allow cheaper and quicker operations compared to conventional techniques because of a tool-less
134 operation.

135 The Fused Deposition Modeling (FDM) process [20] is one of the most common AM processes.
136 It consists of material deposition line by line, building many layers until the target volume is achieved.
137 A thermoplastic filament in the form of thin wires is used as the base material which passes through
138 a set of feeding rollers into the liquefier [21, 22]. The plastic is heated to its melting temperature
139 with the help of heaters and squeezed out of the nozzle tip, with typical diameter between 0.2
140 and 0.8 mm. This process can produce complex parts with the help of support structures. Multi-
141 material fabrication, to combine different materials in different orientations, is also possible. The
142 advantages of this method are: fast production, ability to print transparent materials, simultaneous
143 multi-material printing, and ability to treat standard polymers and low cost. The basic principle of
144 the FDM process is shown in fig. 2. FDM has a strong potential for successfully producing plastic
145 scintillator detectors with complex geometries.

146 In summary, if additive manufacturing of multiple materials can be successfully used for plastic
147 scintillator, it will allow to produce detectors similar to the 3D-cube scintillator detector described
148 in sec. 3 easily as a single block of material, where the pattern of active scintillator volumes
149 covered by an optical reflector is handled directly by the 3D printer. Since current 3D printers can
150 definitely make object bigger than $20 \times 20 \times 20 \text{ cm}^3$, more than 8,000 cubes of 1 cm^3 each could
151 be manufactured at the same time.

152 **4 3D-printing of polystyrene-based scintillator**

153 Initial trials for 3D printing of scintillators were done using the stereolithographic technique [23]
154 or fused deposition modeling [24]. Although these showed for the first time the strong potential of
155 this approach, the quality was not good enough for applications such as for particle detectors.

156 Our goal is to apply the FDM process to 3D print polystyrene scintillator objects. This strategy
157 profits from the fact that FDM is a well established technique that can easily 3D print multimaterials,

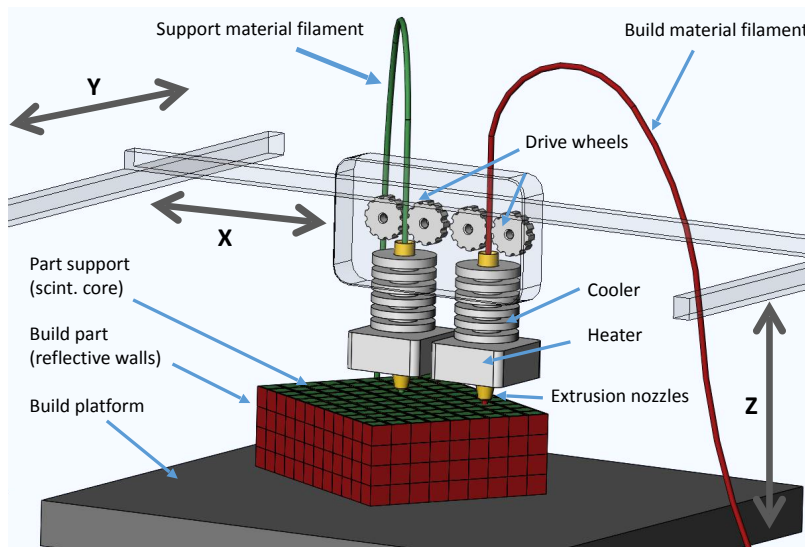


Figure 2: Representation of the FDM process.

158 mandatory for tracking detectors with components that need optical isolation. Moreover, polystyrene
 159 is a very common scintillator material used in most of the high-energy physics experiments, with
 160 perfect quality characteristics for particle detectors, like a large amount of scintillation light yield,
 161 excellent transparency, a fast scintillation process and last but not least, a low cost.

162 The first test showing the potential of the FDM process was done by simply melting pre-
 163 machined polystyrene scintillator. The obtained good transparency indicated that FDM could
 164 be used with polystyrene scintillator. Indeed it was known that polystyrene can be 3D printed,
 165 however it was not clear whether sufficient transparency could be obtained. It was also found that
 166 temperatures of around 200°C allowed to melt the scintillator without degradation of the material
 167 properties. Reducing impurities or the presence of air to avoid oxidation helps to improve the
 168 performance.

169 The preparation for FDM includes the production of the filament and the optimisation of the
 170 FDM printer parameters. At the end, during this study, different polystyrene scintillator cubes were
 171 produced and tested.

172 **4.1 Filament production**

173 The plastic scintillator filament is made of polystyrene doped with 2% by weight of p-terphenyl
 174 (PTP) and 0.05% by weight of 2,2- p-phenylene-bis(5-pheniloxazole) (POPOP). It was obtained
 175 by using an extruder, shown in fig. 3. The main challenge in the FDM filament production is the
 176 hardness of polystyrene, causing the 3D-printer rollers to crush the filament when inserted, or to
 177 produce cracks in the filament when positioning the 3D-printer extruder before starting the process.
 178 Moreover, a pure polystyrene filament cannot be rolled on a standard spool.

179 To overcome this problem, different solutions were tested. We tried to produce the filament
 180 from a copolymer of styrene and butadiene, i.e. styrene-butadiene-styrene thermoplastic elastomers
 181 (SBS TPE plastic). The butadiene makes the plastic more flexible. However, POPOP and PTP are



Figure 3: Picture of the extruder used to produce the scintillator filament.

182 poorly soluble in this plastic and, as a consequence, the scintillator light yield is reduced down to
183 40% of the standard polystyrene scintillator.

184 A second solution consists of adding a plasticizer component to the polystyrene, to increase the
185 mobility of structural elements in the polymer by reducing the crystallizability, the van der Waals
186 surface energy (intermolecular forces between polymer chains), the glass transition temperature
187 and rigidity. It also increases the toughness, i.e. the ability of a material to absorb energy and
188 plastically deforming without creating fractures. After the copolymerization, a flexible filament can
189 be obtained.

190 The selection of the plasticizer was made according to: flexibility, transparency, light yield
191 and long-life of the plastic scintillator. Drawbacks could potentially be the loss of transparency, the
192 aging and the loss of light output. The plastic samples were produced with the cast technology and
193 different types of plasticizer were tested. Fig. 4 shows the different types of plasticizer that were
194 tested. The Compton edge of the spectra obtained by exposing different scintillator samples to a
195 ^{137}Cs γ -source was measured and used to compare the relative light yield.

196 It was found that adding about 5% by weight of biphenyl can achieve the goals, with a light
197 output better than 95% compared to pure scintillator. In fig. 5 the light yield measured from
198 scintillator samples with different biphenyl contents is shown. The concentration of biphenyl
199 has no particular impact on the plastic scintillator transparency. According to data, the obtained
200 mechanical properties of scintillator filament produced by hot extrusion do not considerably depend
201 on the biphenyl content in the polystyrene matrix. Other plasticizer, like DOP and ethylbenzene,
202 were tested. However, it was found that already 5% by weight of the first reduces the scintillation
203 light yield by approximately 30%, although providing good transparency, whilst the latter drastically
204 increase the opacity of the scintillator.

205 Finally, a filament with a diameter of 1.75 mm made of polystyrene-based plastic scintillator
206 with an addition of 5% by weight of biphenyl was produced and used for 3D-printing. Photographs
207 of the polystyrene scintillator filament are shown in fig. 6.

208 4.2 3D-printing process

209 Different samples of plastic scintillator were produced with both “Roboze One+400” [25] and
210 “CreatBot Dx2” [26] printers. Overall both printers provided satisfying results, although the cubes

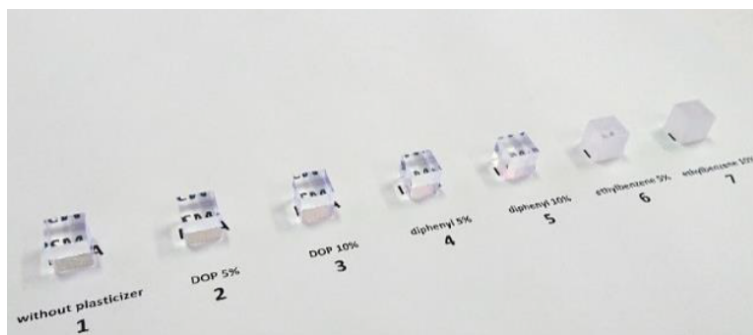


Figure 4: Cubes of cast plastic scintillator with an addition of different plasticizer, in the following order from left to right: without plasticizer, 5% DOP, 10% DOP, 5% byphenil, 10% byphenil, 5% ethylbenzene, 10% ethylbenzene. The fractional amount of plasticizers is by weight.

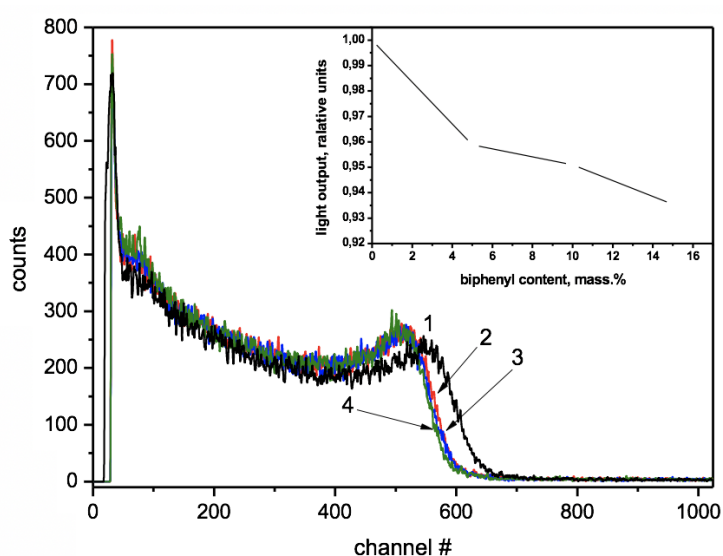


Figure 5: The pulse height spectra of polystyrene-based plastic scintillator exposed to a ^{137}Cs γ -source is shown. The X axis shows the number of ADC channels. Different byphenil compositions by weight were tested: standard composition plastic scintillator (1 - black), 5% biphenyl (2 - red), 10% biphenyl (3 - blue), 15% biphenyl (4 - green). The inset plot on top right shows the dependence of the relative light output as a function of the byphenil content.

211 used for the final tests were produced with the “CreatBot Dx2”. The polystyrene scintillator filament
 212 was produced following the method described in sec. 4.1.

213 Important tuning parameters are the ratio between the extruder diameters and the layer thickness,
 214 the line overlap, the printing speed and the extruder flow. After a campaign of tuning all of those
 215 parameters, a fully dense and transparent scintillator cube was produced. The FDM extruder
 216 diameter was set to the range between 0.4 mm and 0.6 mm. Extrusion temperatures between
 217 240°C and 250°C and printer bed temperatures around 100°C were tested. The printing speed
 218 was between 10 mm/s to 30 mm/s, with a layer thickness between 0.1 to 0.2 mm. In fig. 7 two
 219 polystyrene scintillator cubes are shown during the 3D-printing process.



Figure 6: Photographs of the polystyrene-based scintillator filament used for 3D-printing with the FDM technique. On the right picture, the filament was illuminated with UV light.

220 In the tests the priority was given to the optimisation of the scintillator transparency. It
221 was found that increasing the temperature of chamber, bed and extruder improves the scintillator
222 transparency. On the other hand, the cubic shape is better preserved when not too high temperatures
223 are used. Although improvements of the geometrical shape have not been optimised yet, the cubes
224 could be produced with an edge tolerance of about 0.5 mm. Possible further studies for future tests
225 are discussed in sec. 6.

226 Challenges are possible presence of small air bubbles or not fully-melted zones, that can be a
227 potential source of scintillation light scattering and diffusion inside the scintillator cube. In fact, this
228 could worsen the scintillation light output uniformity within the cube or introduce some opacity. We
229 found that increasing the printer extrusion temperature can minimise these features: the viscosity
230 of the material drops down, the material flows better to the previous printed line with capillary and
231 gravitational forces, the gaps are fully filled and air bubble are minimised.

232 While the inner core of the scintillator cube typically showed a very good transparency, it was
233 noted that the outer surface was more opaque. A particular feature of the FDM technique is the
234 quite high roughness of the outer surfaces vertical with respect to the 3D printer bed. This is due
235 to the visible pattern of the melted filament that makes the outer part of the cube less transparent.
236 Reducing the layer thickness would squeeze the melted polystyrene and improve the transparency.
237 Although more studies will be performed, this feature will not be a particular issue for detectors
238 similar to 3D-cube scintillator where the active volume has to be covered by an opaque or reflecting
239 surface. Moreover, this effect is found only on the outermost surface of the printed scintillator,
240 preventing the inner part (either scintillator or reflector) from being affected by this feature.

241 In order to measure the scintillator light output, the outer surface was polished leading to
242 a slightly smaller cube. In fig. 8 the 3D printed scintillator cube is shown before and after the
243 polishing.

244 **5 Performance of the 3D printed scintillator**

245 The performance of the 3D printer polystyrene scintillator was evaluated by measuring the scin-
246 tillation light yield and counting the number of photons produced per amount of energy deposited

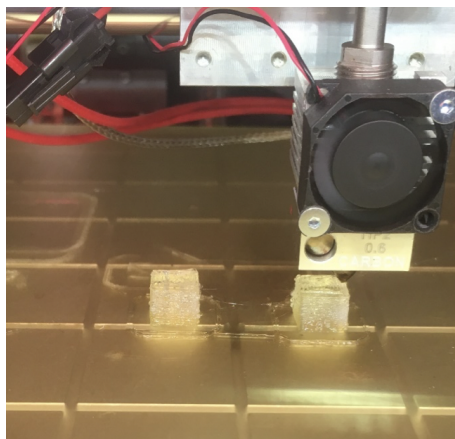


Figure 7: 3D-printing of the plastic scintillator cubes.

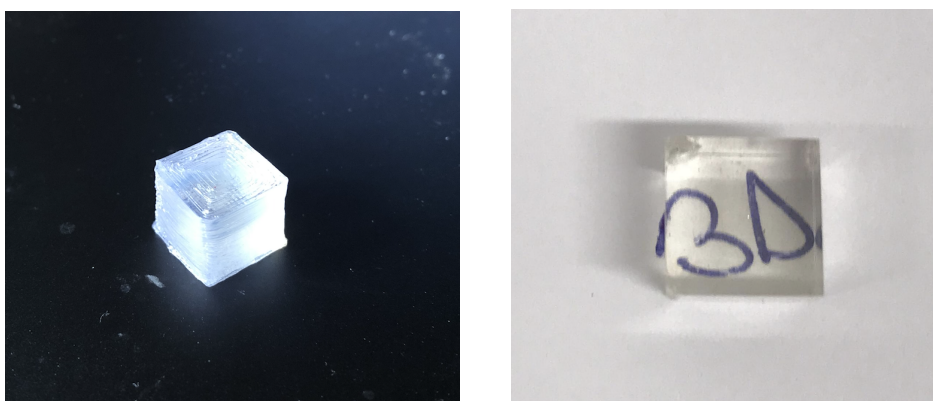


Figure 8: 3D-printed plastic scintillator cube before (left) and after (right) polishing its outer surface.

247 by charged particles. The scintillator cube was 3D printed with “CreatBot Dx2”. The extrusion
 248 diameter was 0.4 mm, the extrusion and bed temperatures respectively 245°C and 100°C. The layer
 249 thickness was 0.1 mm, while the 3D printing speed was 13 mm/s. After polishing the outer surface
 250 the cube has a size of approximately $9 \times 9 \times 9 \text{ mm}^3$, as described in sec. 3.1.

251 The scintillation light yield was measured with Hamamatsu S13360-1350CS Multi-Pixel Pho-
 252 ton Counter (MPPC). The number of photoelectrons (p.e.) was extracted after measuring the MPPC
 253 gain, defined as the number of ADC counts to the number of p.e. conversion. The MPPC active
 254 region ($1.3 \times 1.3 \text{ mm}^2$) was directly coupled with the polystyrene scintillator cube with a black
 255 optical connector, as shown in fig. 9. A piece of soft black EPDM foam was placed inside the
 256 connector to push the cube against the MPPC, improving the coupling. The MPPC charge signal
 257 was read-out with a CAEN DT5702 front-end board [29]. This setup allows to measure mostly the
 258 direct light produced by the scintillator, whilst limiting the light reflection on the outer surfaces
 259 because the inner surface of the optical connector as well as the EPDM foam are black. Hence, the
 260 impact of the light attenuation is mitigated.

261 The scintillator cube was exposed to a strontium-90 source (^{90}Sr). It emits electrons with

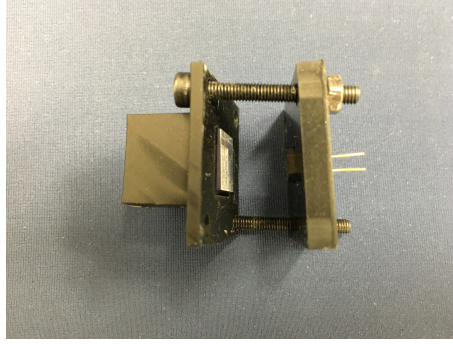


Figure 9: The black optical connector used to couple the MPPC with the scintillator cube is shown. The connector host the cube in a cubical hole. A 5 mm thin piece of EPDM foam is placed inside the connector hole to push the cube toward the MPPC active surface and improve the coupling. The connector was made with a stereolithography 3D printer.

262 energies up to 0.5 MeV through inverse- β decay process, producing a yttrium-90 isotope (^{90}Y)
263 that would further decay to zirconium-90 (^{90}Zr), producing an electron and an antineutrino in the
264 final state. Being a three-body decay the electron can take energies mostly between 0.5 MeV and
265 2.28 MeV [27, 28]. The source was placed on top of the optical connector, opposite of the side
266 with respect to the MPPC position (left side of the picture in fig. 9). Given the optical connector
267 thickness of 2 mm, made of plastic material, mostly electrons from ^{90}Y and with energies above
268 1 MeV are expected to be able to deposit light in the scintillator cube.

269 The light output performance was compared with that of plastic scintillator cubes produced
270 with standard techniques, such as extrusion and cast (see sec. 3.1 for a detailed description), by the
271 “Institute for Scintillation Materials of the National Academy of Science of Ukraine” (ISMA). The
272 cast and extruded plastic scintillator samples consisted of about $10 \times 10 \times 10 \text{ mm}^3$ cubes. It is worth
273 mentioning that the scintillator composition of the cubes produced with different techniques was
274 the same. The measured light yield of the 3D printed scintillator cube is shown in fig. 10. A mean
275 of approximately 12 p.e. was measured. The same light yield was measured with the scintillator
276 cubes produced using the cast and extrusion techniques, and both show energy spectra very similar
277 to the one in fig. 10.

278 An independent measurement of the light yield was performed by collecting cosmic data to
279 confirm the results obtained with the ^{90}Sr source. Cosmic particles deposit about 2 MeV/cm in
280 plastic scintillator. The same setup as for the ^{90}Sr source test was used. In fig. 11 the energy
281 spectra, obtained by the 3D-printed, extruded and cast polystyrene-based scintillator samples, are
282 compared. The spectra were fitted with a Landau function, excluding the low-energy region largely
283 contaminated by environmental photons. It was found that the 3D-printed scintillator shows a light
284 yield similar to the one obtained with the extruded and cast samples, confirming the results of
285 the ^{90}Sr source test. The most probable and width values of the fitted Landau distribution of the
286 3D-printed cube are slightly smaller than the ones from extruded and cast samples, as shown in
287 table 1. Additional uncertainties on the measured parameters could be introduced by environmental
288 photons contaminating the region dominated by cosmic particles. These results are consistent with
289 the ^{90}Sr source ones within the systematic uncertainties of the measurement.

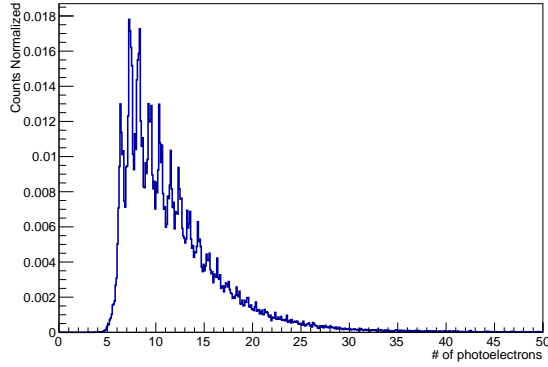


Figure 10: Normalized energy spectrum measured by exposing the 3D printed polystyrene scintillator cube to a ^{90}Sr source. Counts as a function of the number of MPPC p.e. is shown. The peaks correspond to different numbers of p.e. The mean number of p.e. is about 12.

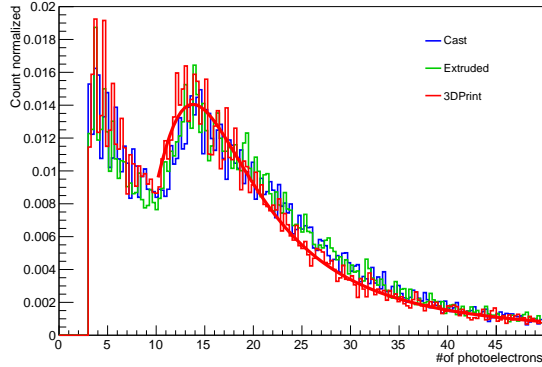


Figure 11: Spectrum of cosmic muons obtained with cast (blue), extruded (green) and 3D printed (red) cubes. For illustration purpose the 3D printed cube data is fitted with a Landau function (red curve). A cut of 3 p.e. was applied to get rid of electronic noise and dark count rate from the spectrum.

Table 1: Parameters obtained by fitting the cosmic data in fig. 11 with a Landau function.

	Most Probable Value (p.e.)	Width (p.e.)
Cast	15.5	3.7
Extruded	15.4	3.7
3D print	14.5	3.3

290 Although the measured number of photoelectrons can be affected by differences in the exper-
 291 imental setup (e.g. cubes size, potentially different quality of the cube surface polishing or small
 292 differences in the coupling between the cube and the MPPC, etc.) and that a limited number of

293 samples has been tested, we can assert that we were able to 3D print polystyrene scintillator of
294 relatively good quality with light yield performance similar to the ones available on the market
295 and widely used (and required) for particle detectors. It is worth mentioning that this experimental
296 setup does not aim to evaluate the effect of the attenuation length in scintillator to the overall light
297 output; this will be measured in future tests.
298

299 **6 Conclusions**

300 In this article we proved the possibility of 3D printing a polystyrene-based scintillator with fused
301 deposition modeling. This process requires both materials and production techniques that are
302 commercially available and is potentially optimal for constructing detectors made of complicated
303 geometries. The scintillation performances of this material are very well known and described in
304 literature.

305 We developed the entire process, including the production of the filament made of polystyrene
306 scintillator and the tuning of the 3D printing parameters. We found that melting polystyrene
307 scintillator does not significantly deteriorate neither the transparency nor the light yield. The
308 scintillation light yield was found to be comparable to the one given by cast or extruded scintillator,
309 based on a limited number of samples that were tested. A detailed characterisation of the 3D printed
310 scintillator will be performed in the future with a large number of samples to test the reproducibility
311 and precisely measure the scintillator properties, such as attenuation length, time decay constant
312 and aging effects.

313 In order to be able to 3D print a particle detector made of 3D-cube scintillator, as described
314 in sec. 3, further R&D steps are needed. First, the scintillator attenuation length will be studied,
315 with attempts of improving it whilst maintaining good geometrical tolerances. Optimisations
316 will be made on the tuning of operational parameters such as the printer bed, room and extruder
317 temperatures. A further step will be the simultaneous 3D printing of scintillator and optical reflector.
318 Finally, the cube will have to be made with holes along the three orthogonal directions to host the
319 WLS fibers.

320 The results reported in this article are a first milestone of an ongoing R&D program which
321 aims to adopt an additive manufacturing techniques for the production of scintillator-based particle
322 detectors.

323 **Acknowledgments**

324 We thank Gianmaria Collazuol for fruitful discussions.

325 **References**

- 326 [1] M. G. Schorr and F. L. Torney, Phys Rev, 1950, 80, 474-474
327 [2] P.A. Amaudruz et al., “The T2K Fine-Grained Detectors”, Nucl.Instrum.Meth. A696 (2012) 1-31
328 [3] C. Joram et al., “LHCb Scintillating Fibre Tracker Engineering Design Review Report: Fibres, Mats
329 and Module”, CERN-LHCb-PUB-2015-008, 03/2015

- 330 [4] V. Andreev et al., “A high-granularity plastic scintillator tile hadronic calorimeter with APD readout
331 for a linear collider detector”, Nucl.Instrum.Meth.A564:144-154,2006
- 332 [5] K.Abe et al., “The T2K experiment”, Nucl. Instrum. Meth. A 659, 106 (2011)
- 333 [6] L. Aliaga et al., “Design, Calibration and Performance of the MINERvA Detector”, Nucl. Inst. and
334 Meth. A743 (2014) 130
- 335 [7] D.G. Michael et al., "The magnetized steel and scintillator calorimeters of the MINOS experiment,"
336 Fermilab-Pub-08-126, Nucl.Instrum.Meth.A596:190-228(2008), Issue 2, 1 November 2008,
337 arXiv:0805.3170
- 338 [8] L. Munteanu et al., “A new method for an improved anti-neutrino energy reconstruction with
339 charged-current interactions in next-generation detectors”, arXiv:1912.01511 [physics.ins-det]
- 340 [9] Y. Abreu et al. (SoLID Collaboration), “Performance of a full scale prototype detector at the BR2
341 reactor for the SoLid experiment”, 2018 JINST 13 P05005
- 342 [10] T. Foerster, Ann. Phys. 2, 55 (1948)
- 343 [11] J. B. Birks, Nuclear Science, IRE Transactions on, 1960, 7, 2-11.
- 344 [12] J. B. Birks, “The theory and practice of scintillation counting”, Pergamon Press; [distributed in the
345 Western Hemisphere by Macmillan, New York], Oxford, New York, 1964.
- 346 [13] A. Blondel et al., JINST 13, P02006 (2018), 709, arXiv:1707.01785 [physics.ins-det].
- 347 [14] C.A. Harper and E.M. Petrie, “In Plastics Materials and Processes: A Concise Encyclopedia” (2003),
348 John Wiley & Sons
- 349 [15] G.S. Atoian, et. al., Nucl. Instr. and Meth. A 531, 467 (2004)
- 350 [16] R. Appel et. al., Nucl. Instr. and Meth. A 479, 349 (2002)
- 351 [17] J.C. Thevenin, L. Allemand, E. Locci, P. Micolon, S. Palanque and M. Spiro, “Extruded polystyrene,
352 a new scintillator”, Nucl. Instrum. Meth. A 169 (1980) 53
- 353 [18] Anna Pla-Dalmau, Alan D. Bross and Kerry L. Mellott, “Low-cost extruded plastic scintillator”, Nucl.
354 Instrum. Meth. A 466 (2001) 482
- 355 [19] S.T. Newman, Z. Zhu, V. Dhokia, and A. Shokrani, “Process planning for additive and subtractive
356 manufacturing technologies,” CIRP Ann. - Manuf. Technol., vol. 64, no. 1, pp. 467-470, 2015.
- 357 [20] “FDM Technology, About Fused Deposition Modeling” (copyright by Stratasys)
358 <http://www.stratasys.com/3d-printers/technologies/fdm-technology>. [Accessed: 26-Mar-2017].
- 359 [21] M. P. Groover, Fundamentals of modern manufacturing: materials, processes, and systems. John
360 Wiley & Sons, Inc, 2013
- 361 [22] A. Bellini and S. Güçeri, “Mechanical characterization of parts fabricated using fused deposition
362 modeling”, Rapid Prototyp. J., vol. 9, no. 4, pp. 252-264, 2003.
- 363 [23] Mishnayot, Y. and Layani, M. and Cooperstein, I. and Magdassi, S. and Ron, G., “Three-dimensional
364 printing of scintillating materials”, Rev.Sci.Instrum. 85 (2014) 085102, ArXiv:1406.4817
- 365 [24] M. Hamel and G. Leboutteiller, “Attempting to prepare a plastic scintillator from a biobased
366 polymer”, J. Appl. Polym. Sci. 2020, 137, 48724.
- 367 [25] <https://www.roboze.com/en/3d-printers/roboze-one-400.html>
- 368 [26] <https://www.creatbot.fr/>

- 369 [27] Dixon, J., Rajan, A., Bohlemann, S. et al. "Evaluation of a Silicon ^{90}Sr Betavoltaic Power Source" Sci
370 Rep 6, 38182 (2016)
- 371 [28] M. Sadeghia, S. Yektab, H. Ghaedic and E. Babanezhadb, "MnO₂ NPs-AgX zeolite composite as
372 adsorbent for removal of strontium-90 (^{90}Sr) from water samples: Kinetics and thermodynamic
373 reactions study", Materials Chemistry and Physics 197 (2017) 113-122
- 374 [29] <https://www.caen.it/products/dt5702/>